European Heart Journal (2011) **32**, 2830–2840
doi:10.1093/eurheartj/ehr059

BASIC SCIENCE

Injectable living marrow stromal cell-based autologous tissue engineered heart valves: *first experiences with a one-step intervention in primates*

Benedikt Weber[1,2,3†], Jacques Scherman[4,5†], Maximilian Y. Emmert[1,2,3†], Juerg Gruenenfelder[2,3], Renier Verbeek[5], Mona Bracher[5], Melanie Black[5], Jeroen Kortsmit[5], Thomas Franz[5], Roman Schoenauer[1,2], Laura Baumgartner[1,2], Chad Brokopp[1,2], Irina Agarkova[1,2], Petra Wolint[1,2], Gregor Zund[1,2], Volkmar Falk[3], Peter Zilla[4,5], and Simon P. Hoerstrup[1,2,3*]

[1]Swiss Center for Regenerative Medicine, Zurich, Switzerland; [2]Department of Surgical Research, University Hospital of Zurich, Zurich, Switzerland; [3]Clinic for Cardiovascular Surgery, University Hospital of Zurich, Raemistrasse 100, 8091 CH-Zürich, Switzerland; [4]Chris Barnard Division of Cardiothoracic Surgery, Groote Schuur Hospital, University of Cape Town, Cape Town, South Africa; and [5]Cardiovascular Research Unit, Cape Heart Centre, University of Cape Town, Cape Town, South Africa

Received 5 November 2010; revised 7 January 2011; accepted 7 February 2011; online publish-ahead-of-print 17 March 2011

This paper was guest edited by Prof. Stephan Janssens, University Hospital Gasthuisberg, Leuven, Belgium.

Aims A living heart valve with regeneration capacity based on autologous cells and minimally invasive implantation technology would represent a substantial improvement upon contemporary heart valve prostheses. This study investigates the feasibility of injectable, marrow stromal cell-based, autologous, living tissue engineered heart valves (TEHV) generated and implanted in a one-step intervention in non-human primates.

Methods and results Trileaflet heart valves were fabricated from non-woven biodegradable synthetic composite scaffolds and integrated into self-expanding nitinol stents. During the same intervention autologous bone marrow-derived mononuclear cells were harvested, seeded onto the scaffold matrix, and implanted transapically as pulmonary valve replacements into non-human primates ($n = 6$). The transapical implantations were successful in all animals and the overall procedure time from cell harvest to TEHV implantation was 118 $\pm$ 17 min. *In vivo* functionality assessed by echocardiography revealed preserved valvular structures and adequate functionality up to 4 weeks post implantation. Substantial cellular remodelling and in-growth into the scaffold materials resulted in layered, endothelialized tissues as visualized by histology and immunohistochemistry. Biomechanical analysis showed non-linear stress–strain curves of the leaflets, indicating replacement of the initial biodegradable matrix by living tissue.

Conclusion Here, we provide a novel concept demonstrating that heart valve tissue engineering based on a minimally invasive technique for both cell harvest and valve delivery as a one-step intervention is feasible in non-human primates. This innovative approach may overcome the limitations of contemporary surgical and interventional bioprosthetic heart valve prostheses.

Keywords Minimally invasive • Heart valve • Tissue engineering • Bone marrow • Stem cells • Primate model

Introduction

Valvular heart disease represents a major cause of morbidity and mortality worldwide.[1] Besides conventional treatment modalities based on surgical valve repair or replacement, the recent clinical implementation of minimally invasive implantation techniques is expected to have a major impact on the management of patients with valvular heart disease.[2] Various percutaneous catheter-based

† These authors contributed equally to this paper.

* Corresponding author. Tel: +41 44 255 3644, Fax: +41 44 255 4369, Email: simon_philipp.hoerstrup@usz.ch

as well as transapical surgical implantation approaches have been developed and successfully used in both experimental and clinical settings, representing a promising alternative to conventional heart valve surgery.[3–5] However, despite these auspicious therapeutic advances, currently available valvular substitutes for minimally invasive replacement procedures are bio-prosthetic and as such inherently prone to calcification and progressive dysfunctional degeneration suggesting their primary clinical application in elderly patients.[6]

Living autologous heart valve substitutes with regeneration and growth potential could overcome the limitations of today's valvular prostheses and enable the application of minimally invasive treatment modalities to a broader patient population, including young patients.[7] We recently demonstrated the principal feasibility of merging the two innovative heart valve replacement technologies of heart valve tissue engineering (HVTE) and minimally invasive delivery in an ovine model.[8] A clinically relevant HVTE concept ideally comprises minimally invasive techniques for both cell harvest and valve delivery. Therefore, several potential cell sources and protocols have been assessed;[9–12] however, most of them requiring an extensive and complex *ex vivo* cell and tissue culture phase. Shińoka *et al.*[13–17] described a method of creating tissue-engineered vascular grafts (TEVG) by using bone marrow-derived mononuclear cells (BMCs) without cell expansion culture. Constructed from biodegradable polyester tubes seeded with autologous cells, these grafts demonstrated functionality and appeared to transform into living vascular grafts. Initial clinical pilot studies evaluating BMC-seeded vascular grafts as venous conduits for congenital heart surgery revealed adequate safety profiles and functionality up to 8 years.[18–21]

The present study investigates for the first time the implantation of autologous BMC-based tissue engineered heart valves (TEHV) by minimally invasive implantation technologies in a primate model; thereby approximating the human situation as much as possible in a pre-clinical large animal model. The presented autologous approach provides a minimally invasive, one-step heart valve replacement procedure from cell harvest to *in vitro* engineering and transapical delivery of living TEHV.

Methods

Scaffold fabrication

Trileaflet heart valve scaffolds were fabricated from non-woven polyglycolic acid meshes (PGA; Cellon, Luxembourg), coated with 1.75% poly-4-hydroxybutyrate (P4HB; TEPHA, Inc., USA; see Supplementary material online, *Methods A*). Thereafter, the scaffolds were integrated into radially self-expandable nitinol stents (length = 30 mm; OD = 20 mm; pfm AG, Germany) by attaching the scaffold matrix to the inner surface of the nitinol stent wires. After vacuum drying for 24 h, the scaffolds were sterilized overnight by using ethylene oxide (EtO) gas sterilization.

Isolation of primate bone marrow-derived mononuclear cells

A volume of 66.5 ± 14.4 mL of bone marrow was aspirated from the sternum of adult Chacma Baboons into a heparinized syringe (50–100 U/mL) using a 12-Gauge threpine needle. Bone marrow-derived mononuclear cells were obtained by centrifuging the samples on a histopaque density gradient (Sigma Chemical Co., USA) for 30 min at 1500 r.p.m (500 g). The viability of the isolated buffy coat was determined by flow cytometry and Trypan Blue staining after erythrocyte elimination and quantification with a haemocytometer (see Supplementary material online, *Methods B*). All animals received human care and the study was approved by the institutional review boards (Department of Surgery Research Committee: Approval Ref. 2009/096, Animal Research Ethics Committee; Approval Ref. 009/035, Faculty of Health Sciences, University of Cape Town) and in compliance with the Guide for the Care and Use of Laboratory Animals, published by the National Institutes of Health (NIH publication No. 85-23). The transport of explanted tissue for histological analysis was in accordance with the *Convention on International Trade in Endangered Species* (CITES) regulations for transport of protected species (CITES Export Permission No. 091992; Import Permission No. 3710/09). Unseeded controls were not included for ethical reasons given the results of previous experiments in the sheep model. When using the same tissue engineering technology, unseeded (only fibrin-coated) scaffolds implanted in the orthotopic pulmonary position of sheep demonstrated severe structural failure already after 4 weeks (see Supplementary material online, *Figure S1*).

Phenotyping of bone marrow-derived mononuclear cells

Small samples of isolated BMCs of each animal were used for haematoxylin–eosin (H&E) staining and immunocytochemical analysis. The cells were fixed with methanol and immunofluorescence staining was performed using for the following epitopes: CD45, CD34, CD146, CD90, CD166, CD44, and DAPI. Phalloidin Alexa 633 was used as control staining. Primary antibodies were detected with Cyanine-2 or Cyanine-3 goat anti-mouse antibodies (see Supplementary material online, *Methods B* and *C*). In order to evaluate the *in vivo* fate of isolated primate BMCs ($n = 2$) seeded cells were tracked for 4 weeks *in vivo* using the CellTrace™ CFSE Cell Proliferation Kit (C34554, Invitrogen Corp., USA; see Supplementary material online, *Methods D*).

Bone marrow-derived mononuclear cell seeding and characterization

Seeding of the BMCs onto the stented heart valve scaffolds ($8 \pm 3 \times 10^6$ cells/cm^2) was performed using fibrin (Sigma Chemical Co., St. Louis, MO, USA) as a cell carrier.[22] After seeding, the constructs were placed into vented 50 mL tubes for 10 min to allow the fibrin–thrombin solution to clot adequately. Thereafter, the seeded construct was loaded into the delivery device by decreasing the diameter from 20 to 8 mm and transferred to the theatre. Mesenchymal stem cells (MSCs) were obtained from bone marrow aspirate according to the method of Pittenger *et al.*[23] and were differentiated into pre-adipocytic and osteoblastic phenotypes (see Supplementary material online, *Methods J*) to confirm their differentiation potential.

Tissue engineered heart valves implantation and *in vivo* functionality

For evaluation of *in vivo* functionality, TEHV were minimally invasively delivered into the pulmonary valve position using a mini-sternotomy and antegrade transapical approach. The valves were crimped and loaded onto a custom-made inducing system (OD = 8 mm) consisting of a rigid tube and pusher. The right ventricle was punctured using needle through purse-string sutures. Next, the inducer system was inserted and the TEHV was delivered into the pulmonary artery under guidance of fluoroscopy (BV, Pulsera, Philips, Medical Systems,

The Netherlands) and transoesophageal echocardiography (2D-transoesophageal echo cardiography (TEE), Philips, Medical Systems, The Netherlands). The radial expansion of the nitinol stent forced the native pulmonary valve leaflets against the pulmonary artery wall and kept them fixed. One construct was deployed in a supravalvular position not excluding the native valvular leaflets. The appropriate position and functionality of the implanted valve was confirmed by angiography. In addition, the *in vivo* functionality was monitored using transoesophageal, transthoracic, and/or epicardial echocardiography during the procedure, immediately after implantation, weekly up to 4 weeks, and prior to sacrifice of the animal (see Supplementary material online, *Methods E*). The pulmonary artery pressure was measured in order to exclude stent-associated stenosis of the pulmonary outflow tract. Anticoagulation (aspirin and warfarin) was maintained for 4 weeks. The animals were sacrificed (potassium euthanization and exsanguination) after 12 h ($n = 1$) and 4 weeks ($n = 5$) and the TEHV were explanted.

Qualitative explant tissue analysis

Tissue composition of explanted heart valve constructs was analysed qualitatively using immuno-/histology and compared with native heart valve leaflets. The tissue sections were studied using Azan staining, Von Kossa staining, H&E staining, Masson–Trichrome staining, and Elastin-van-Gieson (eVG) staining. In addition, immunohistochemistry was performed using the Ventana Benchmark automated staining system (Ventana Medical Systems, Tuscon, AZ, USA) and antibodies for alpha smooth muscle actin (α-SMA), Desmin, CD 68, CD34, CD31, eNOS, HAM-56, and von Willebrand factor (see Supplementary material online, *Methods F*). Representative tissue samples of TEHV were analysed using Scanning Electron Microscopy (see Supplementary material online, *Methods G*).

Quantitative explant tissue analysis

Explanted TEHV (4 week explants, orthotopical position) were lyophilized and analysed by biochemical assays for total DNA, hydroxyproline (HYP) as well as glycosaminogylcans (GAG) content (see Supplementary material online, *Methods H*). For measuring the DNA amount, the Hoechst dye method[24] was used. The GAG content was determined using a modified version of the protocol described by Farndale *et al.*[25] and a standard curve prepared from chondroitin sulphate from shark cartilage (Sigma Chemical Co., USA). Hydroxyproline was determined with a modified version of the protocol provided by Huszar *et al.*[26] The mechanical properties of the leaflets and the valve conduits were assessed independently in radial direction by uniaxial tensile testing to determine ultimate tensile stress (UTS) as well as Young's modulus (YM; see Supplementary material online, *Methods I*).

Statistical analysis

All quantitative data are presented as mean ± standard deviation (SPSS 17.0, IBM, Somers, NY, USA).

Results

Viable bone marrow-derived mononuclear cells harvested from the sternum: a cocktail of stem cells and leucocytes

The isolation of BMCs rendered 175 ± 82 × 10^6 cells per animal for scaffold seeding. Cellular viability was in excess of 95% as verified by whole-blood flow cytometry (*Figure 1A*) and Trypan Blue exclusion staining (*Figure 1B*). Isolated primate mononuclear cells (*Figure 1C*) stained positively for common leucocytic antigens including CD45, CD44, and CD15 (see Supplementary material online, *Figure S2A–C*). According to the flow cytometric analysis the marrow mononuclear cells comprised distinct leucocytic cell populations including granulocytes (20.8%), monocytes (7.6%), and lymphocytes (67.6%). The amount of dead cells, indicated by a population of low forward scatters (FSC)-height and increased side scatters (SSC)-height in the scatter plot was <5% (*Figure 1A*).

Primate bone marrow aspirate comprised $CD34^+$ haematopoietic stem cells as well as MSCs staining positively for CD44, CD90, CD146, and CD166, but negatively for CD45 and CD34, representing a common staining pattern for MSCs (*Figure 1G* and *H*; see Supplementary material online, *Figure S2D*). The differentiation potential of isolated primate MSCs was assessed exemplarily using pre-adipocytic and osteoblastic differentiation assays (see Supplementary material online, *Figure 2E* and *F*). After isolation, BMCs were labelled (*Figure 1D–F*) and successfully seeded onto PGA/P4HB heart valve scaffolds (*Figure 2A–D*) and the TEHV could be inserted into the sheath system for transapical delivery.

Minimally invasive delivery: the transapical implantation of tissue engineered heart valves

The transapical implantations were successful in all animals. Of all six animals five valves were deployed in the orthotopic valvular position (*Figure 3A–C* and *E*), whereas one valve was positioned supravalvularly thereby not excluding the native valvular leaflets. In one of the orthotopically implanted animals perioperative coronary perfusion complications not related to the TEHV functionality resulted in termination 12 h after implantation. Positioning of the TEHV was verified intraoperatively using TEE and fluoroscopy (*Figure 4C* and *D*; see Supplementary material online, *Trailer S1*). Neither migration of the TEHV nor paravalvular leakage has been observed. Proper opening and closing behaviour was demonstrated by TEE measurements (*Figure 4E–H*; See Supplementary material online, *Trailer S2* and *S3*). The mean crimping time of the TEHV (*Figure 3D* and *A–C*), from insertion into the application system until surgical deployment, was 17 ± 8 min (*Figure 3D* and *E*). The mean duration of the entire procedure, from bone marrow harvest until valve delivery, was 118 ± 17 min.

In vivo performance of tissue engineered heart valves

Valve functionality with leaflet mobility and sufficient opening and closing behaviour was observed after implantation. No paravalvular leakage was detected during the follow-up period. Weekly TTE/TEE follow-up revealed a slight but not significant increase in transvalvular peak pressure (TVG; *Table 1*) starting around 25 ± 7 mmHg (TEE) perioperatively, up to 30 ± 7 mmHg after 3 weeks (TTE). At explantation (4 weeks), TVG gradient was clearly reduced to 16.1 ± 1.9 mmHg (TEE). Moderate regurgitation was detected in three animals, which remained unchanged over the whole period of implantation time until harvest. Proper opening and closing behaviour could be demonstrated by

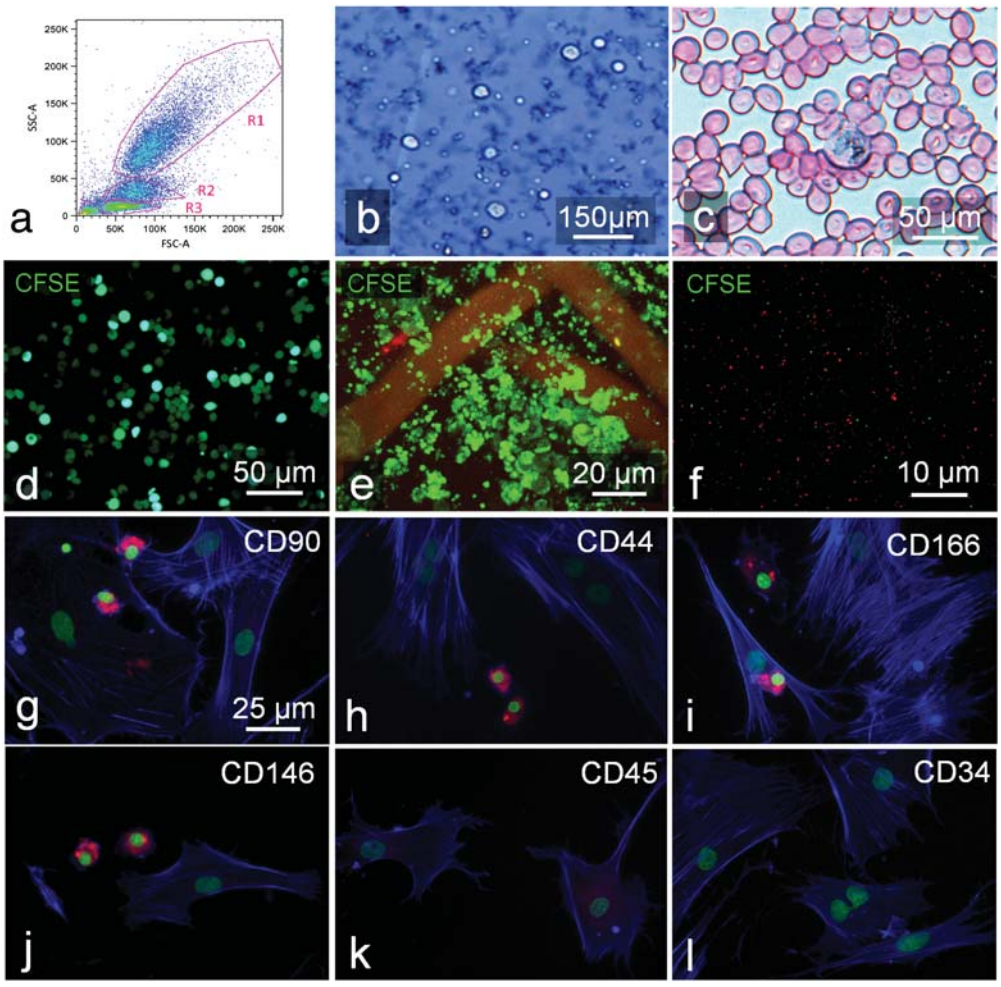

Figure 1 Isolation of bone marrow-derived mononuclear cells. Flow cytometry scatter (*A*) plot of nucleated cells with microfluidic erythrocyte lysis labelled by population with as forward scatters vs. side scatters. The fraction of dead cells, indicated by low forward scatters/high side scatters values, is <5%. This is confirmed by Trypan Blue exclusion staining (TBS; *B*). Mononuclear cells (*C*; H&E staining) were labelled with CFSE (*D*) and seeded onto the polyglycolic acid matrix (*E*). After 4 weeks no fluorescent cells could be detected in the explants tissue (*F*). A fraction of adherent bone marrow-derived mononuclear cells stained positively for CD44, CD90, CD146, CD166, and negatively for CD45 and CD34 indicating a mesenchymal stem cell character (*G*–*L*). Specific staining is shown in red, DAPI (nuclei in green), and Phalloidin (f-actin in blue) were used as control stainings.

TTE/TEE measurements (*Figure 4D–G*; see Supplementary material online, *Trailer S2* and *S3*).

Explant macroscopy of tissue engineered heart valves

Explantation of the early TEHV (12 h) revealed an intact leaflet structure dominated by a fibrin-coated PGA scaffold matrix with lack of evidence for thrombus formation. Harvest of the remaining TEHV 4 weeks after delivery showed constructs that were well integrated into the adjacent tissue-by-tissue covering the stent margin and encircling stent strut endings (*Figure 4A*). The valvular leaflets of the four orthotopically positioned constructs presented as pliable, well-defined cusps (*Figure 4B*). Although the leaflets appeared to be shortened in radial diameter, sufficient co-aptation was demonstrated throughout the entire experimental period. Interestingly, in the haemodynamically non-fully loaded TEHV deployed in the supravalvular position the leaflet structure was almost entirely missing. Instead two small parietal nodes could be identified, most likely representing remnants of the original scaffold pockets (*Figure 4C*).

Scanning electron microscopy

The surface of the early explants (12 h) was mainly characterized by previously seeded mononuclear cells embedded into a fibrin matrix densely covering the entire scaffold (*Figure 5A* and *B*). Analysis of the 4-week explants revealed that three of the orthotopically implanted leaflets showed already a mature structure, characterized by a well-defined endothelial lining on the conduit wall as well as partially on the valvular leaflets (*Figure 5E* and *F*). In several spots these endothelial coverages were confluent and

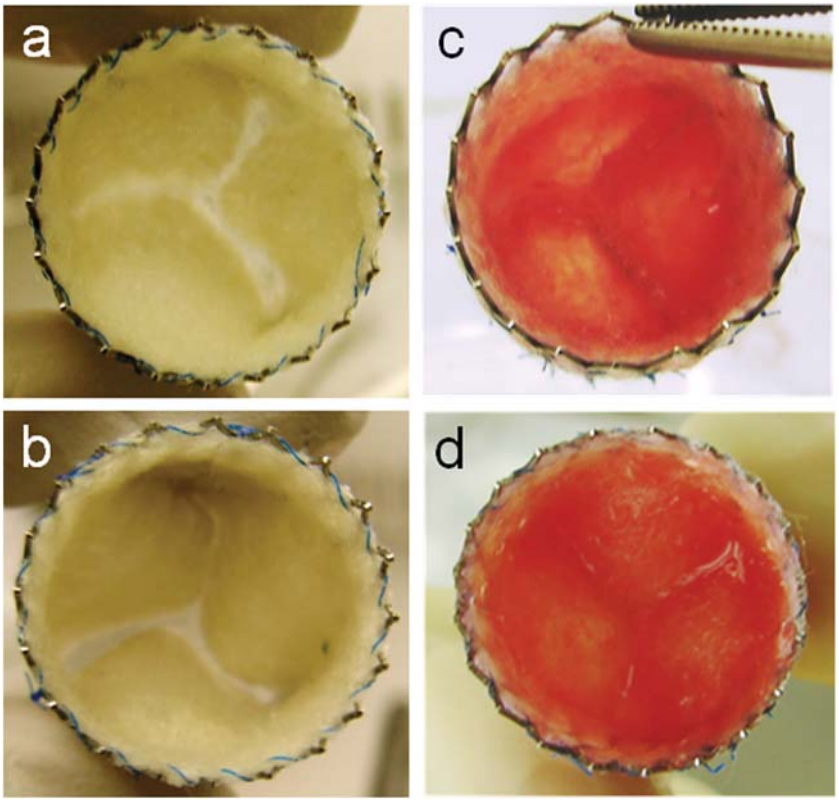

Figure 2 Bone marrow-derived tissue engineered heart valves. After isolation of bone marrow-derived mononuclear cells, stented polyglycolic acid scaffold matrices (*A* and *B*) were seeded with cells using fibrin as a cell carrier (*C* and *D*).

not distinguishable from native primate (*Figure 5C*) or human (*Figure 5D*) valvular endothelium. The other orthotopic explant presented with a more premature surface remodelling, characterized by areas with extensive fibrin formation as well as leucocyte and thrombocyte attachment. Interestingly, in this explant all stages of surface remodelling could be detected, from beginning provisional thrombocyte-mediated surface coverage (*Figure 5G–I*) to areas of almost confluent endothelial covering. The non-orthotopically positioned construct also revealed a well established endothelial coverage with the remaining leaflet structure firmly integrated into the conduit wall.

Histology and immunohistochemistry

Haematoxylin–eosin staining (*Figure 6A–D*) of the explants demonstrated layered tissue morphology, characterized by a central core of non-degraded PGA matrix surrounded by dense tissue formation on the luminal as well as on the vascular side. Masson's Trichrome and eVG staining confirmed the presence of collagen predominantly in the outer layers of the conduit wall and the leaflet (*Figure 6E–L*). As confirmed by SEM, the surface of the conduit was covered by a confluent endothelial layer in large areas of the constructs. Cells of the constructs' surface layer expressed CD31 (*Figure 6M–P*) and vWF, resembling the staining pattern of native valve endothelial cells (*Figure 6M*). Moreover, α-SMA expression could be detected in interstitial cells of the newly formed surface layers of the conduit (*Figure 6S*) and partially of the leaflet (*Figure 6T*). In contrast to previous studies,[8] the leaflets' hinge region was free of α-SMA and/or Desmin positivity (see Supplementary material online, *Figure S3C* and *D*). The early (12 h) as well as the late (4 weeks) explants stained positively for CD68 (see Supplementary material online, *Figure S3G–I*), indicating a distinct monocytic infiltration and continuous remodelling. Cell tracking analysis using CFSE-dye and confocal microscopy (*Figure 1D* and *E*) revealed no signal within the explanted tissue (*Figure 1F*), indicating that most of the seeded BMCs were not present after 4 weeks *in vivo*.

Biomechanical and extracellular matrix analysis: the remodelling of viable tissue

Mechanical evaluation was performed separately for the valvular leaflets and the wall region. Analysis of the 4 week explants revealed that the tissue strength (UTS 0.19 ± 0.12 MPa) as well as the stiffness (YM 1.0 ± 0.54 MPa) of the conduit wall was higher than that of the valvular leaflet itself (UTS 0.08 ± 0.05 MPa; YM 0.19 ± 0.08 MPa). The stress–strain curves of both the heart valve leaflet and the conduit wall revealed non-linear behaviour until rupture. The YM obtained in the low strain (0.0–10.0%) as well as the high strain (>10.0%) showed to be significantly different (all *P*'s <0.05), which is characteristic for properties of biological tissue (see Supplementary material

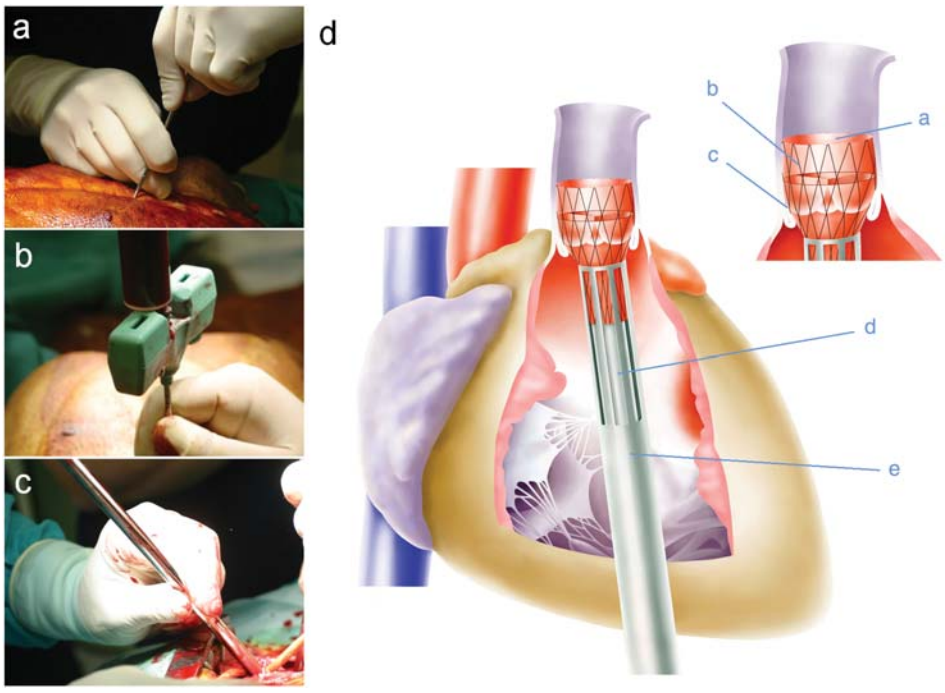

Figure 3 Minimally invasive tissue engineered heart valves implantation. After sternal bone marrow puncture (*A*) and aspiration of fluid (*B*), the tissue engineered heart valve was loaded into the delivery device (*C*), inserted into the right ventricle (*D*) and deployed in the pulmonary position under sonographic and fluoroscopic guidance. The crimped tissue engineered heart valve (a), integrated into the nitinol stent (b), is carefully deployed into the pulmonary position (c) by slowly advancing the inner pusher (d) into the sheath system (e).

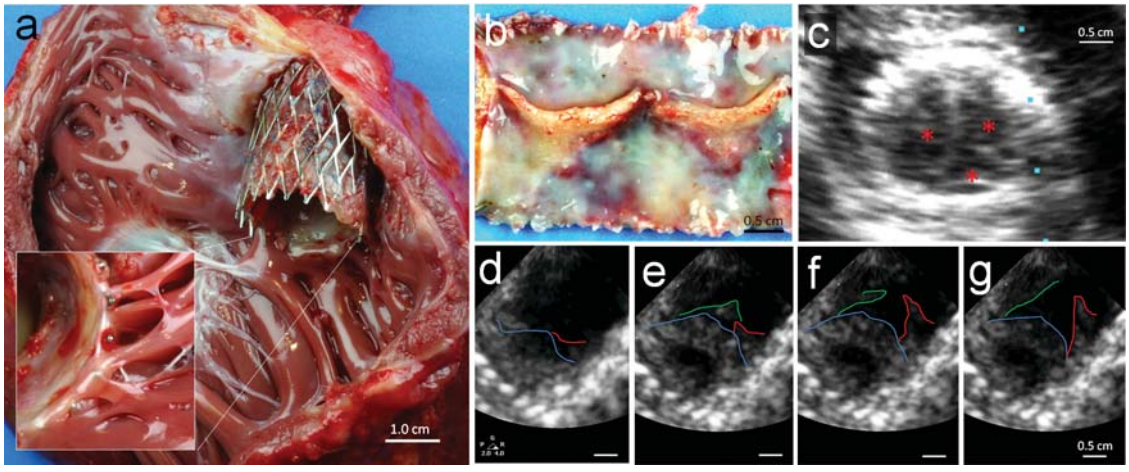

Figure 4 Explant analysis of tissue engineered heart valves. After 4 weeks *in vivo* the stented constructs were well integrated into the adjacent tissue (*A*). Orthotopical tissue engineered heart valves (*B*) presented with a cusp-like leaflet structure, with shorter leaflets than native controls. In a final transoesophageal echocardiography-assessment the leaflet co-aptation (*C*; asterisk indicates leaflets) as well as opening movements of all three leaflets could be visualized (*D*–*G*).

online, *Figure S4*), indicating the *in vivo* replacement of the biodegradable matrix by living tissue (*Figure 7A*).

Quantitative extracellular matrix (ECM) analysis of the TEHV explants showed that the GAG as well as the DNA content of the constructs' leaflets was higher than compared with native tissue (GAG 140.28 ± 36.17%; DNA 168.10 ± 87.07%), indicating high cellular infiltration as well as ECM remodelling. Consistent with previous studies,[8] the collagen content in the leaflets and the conduit wall was substantially lower in the newly formed tissues than compared with native controls (HYP 59.24 ± 16.87%; *Figure 7B*).

Table 1 Transvalvular peak pressure gradient (mmHg), international normalized ratio, and grade of regurgitation during 4 weeks follow-up of orthotopically delivered tissue engineered heart valve (mean ± SD)

Value	1 Week	2 Weeks	3 Weeks	4 Weeks
TVG[a]	26.9 ± 7.5	28.6 ± 5.1	30.4 ± 7.8	16.1 ± 1.9
INR[b]	1.2 ± 2.5	1.5 ± 3.5	1.25 ± 0.13	*Ex*[c]
Regurgitation[d]	2.0 ± 0.7	2.0 ± 0.7	2.5 ± 1.5	2.5 ± 0.9

[a]TVG, transvalvular peak pressure gradient;
[b]INR, international normalized ratio;
[c]*Explantation*;
[d]Regurgitation—Grading: 0/1/2/3/4—None/trivial/mild/moderate/severe.

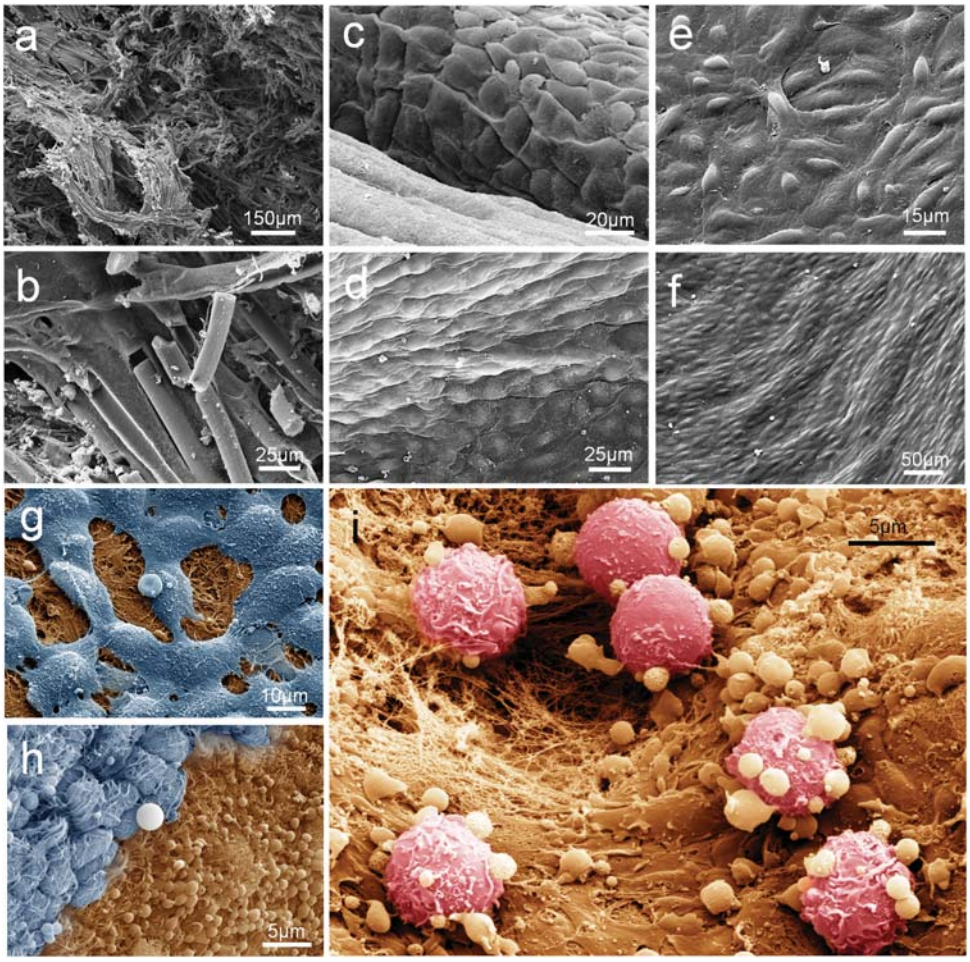

Figure 5 Scanning electron microscopy of the polyglycolic acid–poly-4-hydroxybutyrate scaffold (*A* and *B*), primate (*C*), and human (*D*) control leaflets. In most areas the surface of the 4 week explants showed confluent (*E* and *F*) or initial (*G*) endothelial coverage. In some areas the surface remodelling was still evident involving thrombocyte attachment (*H*) and leucocyte attraction (*I*).

Discussion

Minimally invasive heart valve replacement techniques have recently emerged as a promising technology in interventional cardiovascular therapeutics.[2,6,27,28] Despite the potential of this novel technology, currently used replacement materials for transcatheter or transapical valves are bioprosthetic and therefore highly prone to calcification as well as structural degeneration.[29,30] Living TEHV, based on rapidly biodegrading scaffolds and autologous cells could overcome these limitations with characteristics such as repair, remodelling, and growth. We recently demonstrated the principal feasibility of merging tissue engineering and minimally invasive

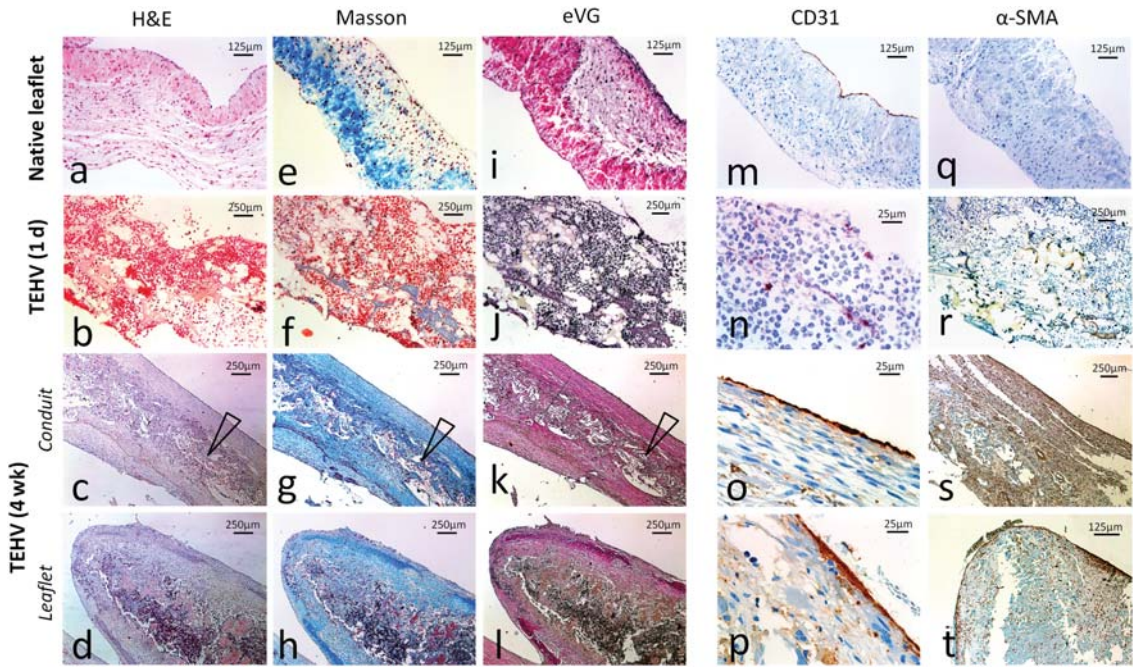

Figure 6 Histology of the explanted living tissue engineered heart valves. Explanted tissues showed layered tissue architecture visualized by haematoxylin–eosin staining (*A–D*). In Masson's Trichrome staining (*E–H*) and Elastin-van-Gieson staining (*I–L*) collagen fibres were predominantly found in the outer tissue layer of the conduit and leaflets. Cells of the conduit (*O*) and leaflet (*P*) surface layer expressed CD31 (*M–P*). α-SMA expression (*Q–T*) could be detected in the outer layers of the conduit (*S*) and the leaflet (*T*), but was missing in the proximal leaflet region. Arrows indicate reminiscent scaffold material.

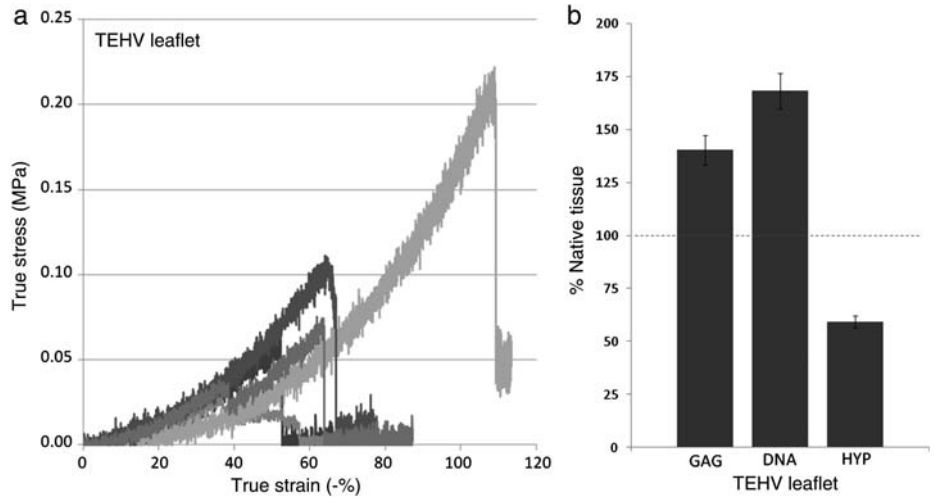

Figure 7 Qualitative tissue analysis. Mechanical properties of explanted tissue engineered leaflets after 4 weeks *in vivo* are displayed as stress–strain curves [MPa/%] characteristic for biological tissue (*A*). Extracellular matrix analysis of the explants for glycosaminogylcans and DNA shows enhanced values compared with native tissues. Hydroxyproline normalized to tissue weight is decreased compared with native controls (*B*).

heart valve replacement technologies.[8] Ideally, a clinically relevant HVTE concept must involve low-invasive techniques for both cell harvest and valve delivery. Consequently, several non-invasive potential cell sources comprising stem cells have been assessed with regard to the clinical realization of the concept. However, most of these concepts require extensive, logistically complex,

and time-consuming *in vitro* tissue engineering processes that limit their clinical feasibility.

The present study demonstrates for the first time the feasibility of merging heart valve tissue engineering based on a low-invasive stem cell source, with a minimally invasive, injectable implantation technology combined in a single intervention. Stem cell sources previously used for HVTE, including MSCs, foetal stem cells, and blood-derived progenitors,[8–12] necessitate cell harvest in a particular intervention, followed by protracted and complex *in vitro* cell expansion and implantation of fabricated TEHV in a second procedure.[8] To the contrary, autologous BMCs can be isolated in sufficient numbers from sternum bone marrow aspirates, thereby enabling immediate re-implantation as autologous TEHV. Therefore, the presented one-step approach suggests a highly clinically relevant concept and may represent a significant step towards the routine utilization of TEHVs.

The principle of using BMCs for cardiovascular tissue engineering was described by Shin'oka *et al.*[13] and has been assessed in preclinical[14–16] as well as initial clinical investigations.[18–21] It was hypothesized that multipotent bone marrow-derived stem cells proliferate, differentiate, and constitute new tissues.[19] In a recent study, Roh *et al.*[17] elucidated the potential underlying molecular mechanism of autologous BMC-induced tissue formation. In contrast to previous assumptions, no evidence for (trans-) differentiation of bone marrow-derived stem cells into mature vascular cells has been found. Interestingly, seeded BMCs were not detectable in the tissue engineered constructs 1 week after implantation. In fact, it was shown that BMC-seeded biodegradable scaffolds transform into functional blood vessels via an inflammation-mediated process of vascular remodelling. While the role of BMCs in this remodelling process remains largely conjectural, a growing body of evidence suggests their role within inflammation-mediated processes.

This paracrine role of seeded BMCs as a constituent of an inflammatory vascular remodelling process is consistent with multiple studies reporting that (trans-)differentiation of bone marrow-derived stem cells *in vivo* is deemed rare.[10,31–36] The present study concurs with this mechanism, as the initially labelled BMCs were not detectable within the explants 4 weeks after implantation. Also, a distinct remodelling process was evident, characterized by a monocytic infiltration of the leaflets as well as the conduit wall. Besides this critical role of seeded BMCs for *in vivo* remodelling and tissue formation,[17,19] the precise contribution of the detectable multipotent BMC stem cell fractions is of great interest to understand the underlying regenerative mechanism.[37–40]

Experimentally, it would have been elegant to include an unseeded control group in this study. However, previous experiments in the sheep model using the same tissue engineering technology and unseeded (only fibrin-coated) scaffolds implanted in the orthotopic pulmonary position demonstrated severe structural failure after 4 weeks (see Supplementary material online, *Figure S1*). Given the fact that remodelling phenomena in the ovine model are expected to be substantially more intense than in the human/primate cardiovascular system,[41] the implantation of unseeded controls into primates appeared ethically not justifiable.

A very interesting observation of the current study was the influence of haemodynamic loading on remodelling, tissue formation, and maturation *in vivo*. This is a known phenomenon from embryology and has been used for *in vitro* tissue engineering experiments utilizing biomimetic flow and pressure conditions to achieve optimal tissue maturation in so-called bioreactors.[42,43] In the present investigation, the role of mechanical loading on functional remodelling was uniquely demonstrated by the supra-valvular positioned TEHV not excluding the native valvular leaflets. In contrast to the orthotopic implants, the non-loaded supravalvular TEHV lacked any leaflet structure after 4 weeks, indicating missing tissue formation as well as BMC-mediated leaflet remodelling.

Macroscopically the orthotopic constructs presented with cusp-like leaflet structures and did not appear thickened compared with previous reports based on the sheep model.[8,44] Although principal valvular functionality was demonstrated, mild to moderate regurgitation was observed by echocardiography in three of five valves in the presence of leaflet co-aptation. This may be explained by the rather prototypic design of the TEHV in this proof of concept study. Furthermore, a minimal structural shortening of the TEHV cusps was detectable which will be addressed in future TEHV scaffold designs e.g. by oversizing of the co-aptation areas of the starter matrices. Further enhancement of cellular attraction and, thus, tissue formation particularly in the distal leaflet region may provide solutions.[45] Finally, following this feasibility study introducing injectable TEHV generated and minimally invasively implanted in a single intervention, extended long-term studies are mandatory in order to further elucidate the fate of such living autologous cell-based engineered heart valves as well as the underlying tissue remodelling mechanisms observed *in vivo*. Particularly, the precise role of seeded stem cells with respect to their function in chemo-attraction and tissue formation has to be systematically assessed. However, addressing these questions was beyond the scope of this pilot-study and will be investigated in future experiments.

Conclusions

These first results of combining minimally invasive valve replacement procedures with heart valve tissue engineering in a single intervention in a preclinical primate model are promising and demonstrate the feasibility of using BMCs for the fabrication of TEHV. Moreover, utilizing the body's natural abilities to regenerate TEHV *in vivo*, may greatly simplify, and improve the clinical feasibility of the autologous cell-based TEHV approach. Such autologous and living heart valves with repair and regeneration capacities may represent the next generation of transcatheter and transapical heart valves overcoming the time limitations of the currently used bioprosthetic valves suggesting their future clinical application also beyond elderly patients.

Supplementary material

Supplementary material is available at *European Heart Journal* online.

Acknowledgements

The authors thank Deon Bezuidenhout, Ronnett Seldon, Elizabeth VanderMerwe, Ursula Steckholzer, Pia Fuchs, Klaus Marquardt and

Silvia Behnke for their technical support, as well as all the members of the Animal Unit, Faculty of Health Sciences, University of Cape Town for their excellent contribution.

Funding

This work was supported by the Swiss South African Joint Research Programme of the State Secretariat for Education and Research, Swiss and South African Governments [EX25-2010], the Research Infrastructure Support Programme [UID 65720], the National Research Foundation and the Department of Science and Technology South Africa, the University Research Committee - University of Cape Town, the Claude Leon Foundation, the Swiss National Science Foundation [32-122273] as well as the 7th Framework Programme, *Life Valve*, European Commission [242008].

Conflict of interest: S.P.H. and G.Z. are scientific advisors of Xeltis AG, Switzerland.

References

1. Supino PG, Borer JS, Preibisz J. The epidemiology of valvular heart disease: a growing public health problem. *Heart Fail Clin* 2006;**2**:379–393.
2. Lurz P, Bonhoeffer P, Taylor AM. Percutaneous pulmonary valve implantation: an update. *Expert Rev Cardiovasc Ther* 2009;**7**:823–833.
3. Asoh K, Walsh M, Hickey E, Nagiub M, Chaturvedi R, Lee KJ, Benson LN. Percutaneous pulmonary valve implantation within bioprosthetic valves. *Eur Heart J* 2010;**31**:1404–1409.
4. Momenah TS, El Oakley R, Al Najashi K, Khoshhal S, Al Qethamy H, Bonhoeffer P. Extended application of percutaneous pulmonary valve implantation. *J Am Coll Cardiol* 2009;**53**:1859–1863.
5. Walther T, Schuler G, Borger MA, Kempfert J, Seeburger J, Rückert Y, Ender J, Linke A, Scholz M, Falk V, Mohr FW. Transapical aortic valve implantation in 100 consecutive patients: comparison to propensity-matched conventional aortic valve replacement. *Eur Heart J* 2010;**31**:1398–1403.
6. Walther T, Simon P, Dewey T, Wimmer-Greinecker G, Falk V, Kasimir MT, Doss M, Borger MA, Schuler G, Glogar D, Fehske W, Wolner E, Mohr FW, Mack M. Transapical minimally invasive aortic valve implantation: multicenter experience. *Circulation* 2007;**611**:I240–I245.
7. Fernandes SM, Khairy P, Sanders SP, Colan SD. Bicuspid aortic valve morphology and interventions in the young. *J Am Coll Cardiol* 2007;**49**:2211–2214.
8. Schmidt D, Dijkman PE, Driessen-Mol A, Stenger R, Mariani C, Puolakka A, Rissanen M, Deichmann T, Odermatt B, Weber B, Emmert MY, Zund G, Baaijens FPT, Hoerstrup SP. Minimally invasive implantation of living tissue engineered heart valves—a comprehensive approach from autologous vascular cells to stem cells. *J Am Coll Cardiol* 2010;**56**:510–520.
9. Hoerstrup SP, Kadner A, Melnitchouk S, Trojan A, Eid K, Tracy J, Sodian R, Visjager JF, Kolb SA, Grunenfelder J, Zund G, Turina MI. Tissue engineering of functional trileaflet heart valves from human marrow stromal cells. *Circulation* 2002;**106**:I143–I150.
10. Sutherland FW, Perry TE, Yu Y, Sherwood MC, Rabkin E, Masuda Y, Garcia GA, McLellan DL, Engelmayr GC Jr, Sacks MS, Schoen FJ, Mayer JE Jr. From stem cells to viable autologous semilunar heart valve. *Circulation* 2005;**111**:2783–2791.
11. Schmidt D, Mol A, Breymann C, Achermann J, Odermatt B, Gössi M, Neuenschwander S, Prêtre R, Genoni M, Zund G, Hoerstrup SP. Living autologous heart valves engineered from human prenatally harvested progenitors. *Circulation* 2006;**114**:I125–I131.
12. Schmidt D, Achermann J, Odermatt B, Breymann C, Mol A, Genoni M, Zund G, Hoerstrup SP. Prenatally fabricated autologous human living heart valves based on amniotic fluid derived progenitor cells as single cell source. *Circulation* 2007;**116**:I64–I70.
13. Hibino N, Shin'oka T, Matsumura G, Ikada Y, Kurosawa H. The tissue-engineered vascular graft using bone marrow without culture. *J Thorac Cardiovasc Surg* 2005;**129**:1064–1070.
14. Matsumura G, Ishihara Y, Miyagawa-Tomita S, Ikada Y, Matsuda S, Kurosawa H, Shin'oka T. Evaluation of tissue-engineered vascular autografts. *Tissue Eng* 2006;**12**:3075–3083.
15. Brennan MP, Dardik A, Hibino N, Roh JD, Nelson GN, Papademitris X, Shinoka T, Breuer CK. Tissue-engineered vascular grafts demonstrate evidence of growth and development when implanted in a juvenile animal model. *Ann Surg* 2008;**248**:370–377.
16. Mirensky TL, Nelson GN, Brennan MP, Roh JD, Hibino N, Yi T, Shinoka T, Breuer CK. Tissue-engineered arterial grafts: long-term results after implantation in a small animal model. *J Pediatr Surg* 2009;**44**:1127–1132.
17. Roh JD, Sawh-Martinez R, Brennan MP, Jay SM, Devine L, Rao DA, Yi T, Mirensky TL, Nalbandian A, Udelsman B, Hibino N, Shinoka T, Saltzman WM, Snyder E, Kyriakides TR, Pober JS, Breuer CK. Tissue-engineered vascular grafts transform into mature blood vessels via an inflammation-mediated process of vascular remodeling. *Proc Natl Acad Sci U S A* 2010;**107**:4669–4674.
18. Shin'oka T, Imai Y, Ikada Y. Transplantation of a tissue-engineered pulmonary artery. *N Engl J Med* 2001;**344**:532–533.
19. Matsumura G, Miyagawa-Tomita S, Shin'oka T, Ikada Y, Kurosawa H. First evidence that bone marrow cells contribute to the construction of tissue-engineered vascular autografts *in vivo*. *Circulation* 2003;**108**:1729–1734.
20. Isomatsu Y, Shin'oka T, Matsumura G, Hibino N, Konuma T, Nagatsu M, Kurosawa H. Extracardiac total cavopulmonary connection using a tissue-engineered graft. *J Thorac Cardiovasc Surg* 2003;**126**:1958–1962.
21. Shin'oka T, Matsumura G, Hibino N, Naito Y, Watanabe M, Konuma T, Sakamoto T, Nagatsu M, Kurosawa H. Midterm clinical result of tissue-engineered vascular autografts seeded with autologous bone marrow cells. *J Thorac Cardiovasc Surg* 2005;**129**:1330–1338.
22. Mol A, van Lieshout MI, Dam-de Veen CG, Neuenschwander S, Hoerstrup SP, Baaijens FP, Bouten CV. Fibrin as a cell carrier in cardiovascular tissue engineering applications. *Biomaterials* 2005;**26**:3113–3121.
23. Pittenger MF, Mackay AM, Beck SC, Jaiswal RK, Douglas R, Mosca JD, Moorman MA, Simonetti DW, Craig S, Marshak DR. Multilineage potential of adult human mesenchymal stem cells. *Science* 1999;**284**:143–147.
24. Cesarone CF, Bolognesi C, Santi L. Improved microfluorometric DNA determination in biological material using 33258 Hoechst. *Anal Biochem* 1979;**100**:188–197.
25. Farndale RW, Buttle DJ, Barrett AJ. Improved quantitation and discrimination of sulphated glycosaminoglycans by use of dimethylmethylene blue. *Biochem Biophys Acta* 1986;**883**:173–177.
26. Huszar G, Maiocco J, Naftolin F. Monitoring of collagen and collagen fragments in chromatography of protein mixtures. *Anal Biochem* 1980;**105**:424–429.
27. Bonhoeffer P, Boudjemline Y, Qureshi SA, Le Bidois J, Iserin L, Acar P, Merckx J, Kachaner J, Sidi D. Percutaneous insertion of the pulmonary valve. *J Am Coll Cardiol* 2002;**39**:1664–1669.
28. Cribier A, Eltchaninoff H, Tron C, Bauer F, Agatiello C, Sebagh L, Bash A, Nusimovici D, Litzler PY, Bessou JP, Leon MB. Early experience with percutaneous transcatheter implantation of heart valve prosthesis for the treatment of end-stage inoperable patients with calcific aortic stenosis. *J Am Coll Cardiol* 2004;**43**:698–703.
29. Coats L, Bonhoeffer P. New percutaneous treatments for valve disease. *Heart* 2007;**93**:639–644.
30. Schoen FJ. Evolving concepts of cardiac valve dynamics: the continuum of development, functional structure, pathobiology, and tissue engineering. *Circulation* 2008;**118**:1864–1880.
31. Zentilin L, Tafuro S, Zacchigna S, Arsic N, Pattarini L, Sinigaglia M, Giacca M. Bone marrow mononuclear cells are recruited to the sites of VEGF-induced neovascularization but are not incorporated into the newly formed vessels. *Blood* 2006;**107**:3546–3554.
32. Murry CE, Soonpaa MH, Reinecke H, Nakajima H, Nakajima HO, Rubart M, Pasumarthi KB, Virag JI, Bartelmez SH, Poppa V, Bradford G, Dowell JD, Williams DA, Field LJ. Haematopoietic stem cells do not transdifferentiate into cardiac myocytes in myocardial infarcts. *Nature* 2004;**428**:664–668.
33. Balsam LB, Wagers AJ, Christensen JL, Kofidis T, Weissman IL, Robbins RC. Haematopoietic stem cells adopt mature haematopoietic fates in ischaemic myocardium. *Nature* 2004;**428**:668–673.
34. Wagers AJ, Sherwood RI, Christensen JL, Weissman IL. Little evidence for developmental plasticity of adult hematopoietic stem cells. *Science* 2002;**297**:2256–2259.
35. Terada N, Hamazaki T, Oka M, Hoki M, Mastalerz DM, Nakano Y, Meyer EM, Morel L, Petersen BE, Scott EW. Bone marrow cells adopt the phenotype of other cells by spontaneous cell fusion. *Nature* 2002;**416**:542–545.
36. Nygren JM, Jovinge S, Breitbach M, Säwén P, Röll W, Hescheler J, Taneera J, Fleischmann BK, Jacobsen SE. Bone marrow-derived hematopoietic cells generate cardiomyocytes at a low frequency through cell fusion, but not transdifferentiation. *Nat Med* 2004;**10**:494–501.
37. Kinnaird T, Stabile E, Burnett MS, Shou M, Lee CW, Barr S, Fuchs S, Epstein SE. Local delivery of marrow-derived stromal cells augments collateral perfusion through paracrine mechanisms. *Circulation* 2004;**109**:1543–1549.

38. Gnecchi M, He H, Liang OD, Melo LG, Morello F, Mu H, Noiseux N, Zhang L, Pratt RE, Ingwall JS, Dzau VJ. Paracrine action accounts for marked protection of ischemic heart by Akt-modified mesenchymal stem cells. *Nat Med* 2005;**11**:367–368.
39. O'Neill TJ IV, Wamhoff BR, Owens GK, Skalak TC. Mobilization of bone marrow-derived cells enhances the angiogenic response to hypoxia without transdifferentiation into endothelial cells. *Circ Res* 2005;**97**:1027–1035.
40. Uemura R, Xu M, Ahmad N, Ashraf M. Bone marrow stem cells prevent left ventricular remodeling of ischemic heart through paracrine signaling. *Circ Res* 2006;**98**:1414–1421.
41. Schoen FJ, Levy RJ. Calcification of tissue heart valve substitutes: progress toward understanding and prevention. *Ann Thorac Surg* 2005;**79**:1072–1080.
42. Hoerstrup SP, Sodian R, Sperling JS, Vacanti JP, Mayer JE Jr. New pulsatile bioreactor for in vitro formation of tissue engineered heart valves. *Tissue Eng* 2000;**61**:75–79.
43. Mol A, Driessen NJ, Rutten MC, Hoerstrup SP, Bouten CV, Baaijens FP. Tissue engineering of human heart valve leaflets: a novel bioreactor for a strain-based conditioning approach. *Ann Biomed Eng* 2005;**33**:1778–1788.
44. Flanagan TC, Sachweh JS, Frese J, Schnöring H, Gronloh N, Koch S, Tolba RH, Schmitz-Rode T, Jockenhoevel S. *In vivo* remodeling and structural characterization of fibrin-based tissue-engineered heart valves in the adult sheep model. *Tissue Eng Part A* 2009;**15**:2965–2976.
45. Lutolf MP, Gilbert PM, Blau HM. Designing materials to direct stem-cell fate. *Nature* 2009;**462**:433–441.

CARDIOVASCULAR FLASHLIGHT

doi:10.1093/eurheartj/ehr240
Online publish-ahead-of-print 15 July 2011

Isolated arrhythmogenic left ventricular cardiomyopathy identified by cardiac magnetic resonance imaging

Ingo Paetsch[1]*, Sebastian Reith[1], Nikolaus Gassler[2], and Cosima Jahnke[1]

[1]Department of Cardiology, University Hospital RWTH Aachen, Pauwelsstrasse 30, 52074 Aachen, Germany and [2]Institute of Pathology and Electron Microscopy Facility, RWTH Aachen University, Aachen, Germany

* Corresponding author. Tel: +49 241 80 89705, Fax: +49 241 80 82131, Email: ipaetsch@ukaachen.de

A 78-year-old man experienced a first-time syncope with fall resulting in raccoon eyes and a single episode of non-sustained ventricular tachycardia (>10 beats) was documented. Creatine kinase and troponin T were only weakly abnormal. Echocardiography and invasive coronary angiography were unremarkable.

Cardiac magnetic resonance (CMR) imaging revealed the presence of intramyocardial fatty spots and streaks of the left ventricular (LV) inferolateral wall and the interventricular septum (arrowheads in *Panel A*, steady-state free precession (SSFP) imaging; *Panels B* and *C*, T2-weighted black blood imaging without and with fat suppression; white arrows in *Panel D*, delayed enhancement imaging with diffuse and streaky intramyocardial signal enhancement; see Supplementary material online, *Movie 1*). Right ventricular morphology and regional and global function were normal. Lipomatous metaplasia of chronic myocardial infarction was ruled out by missing regional subendocardial delayed enhancement. Hence, CMR findings were suggestive of isolated arrhythmogenic dysplasia of the LV.

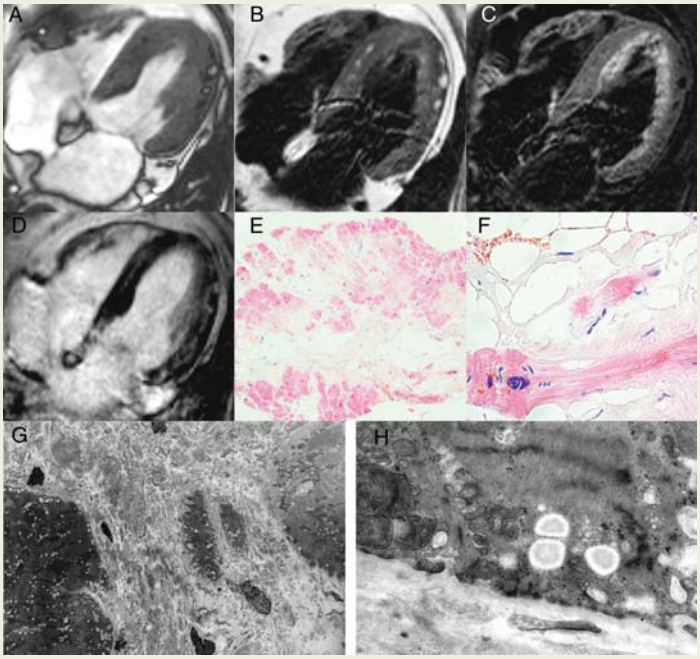

Histopathological work-up including transmission electron microscopy of a deep LV biopsy demonstrated disrupted myocardial architecture with extensive fibrofatty replacement [*Panels E* and *F*, haematoxylin and eosin staining; *Panels G* and *H*, transmission electron microscopy, white arrows indicate cardiomyocytes with several cytoplasmic vacuoles separated by a collagen rich matrix (asterisk); arrowheads, nuclei of fibrocytes; black-lined white arrows, lipid droplets; rectangle in G delineates the magnified image area in *Panel H*].

A 'left-dominant' subtype of arrhythmogenic right ventricular cardiomyopathy (ARVC) has been recognized with multicentre studies reporting LV involvement in ARVC to occur with disease progression in >75% of cases. However, primary LV involvement has been acknowledged as a phenotype expression of ARVC only recently.

Supplementary material: Supplementary material is available at *European Heart Journal* online.